

High-Temperature Guarded Hot Plate Apparatus – Control of Edge Heat Loss

D. R. FLYNN, W. M. HEALY and R. R. ZARR

Revised November 22, 2005

ABSTRACT

The guarded hot plate (GHP) apparatus is the most common type of absolute apparatus for measurement of the thermal transmission properties of thermal insulation. As the name implies, the hot meter plate is surrounded by a coplanar guard plate, separated by a narrow guard gap, that is held at a temperature close (e.g., 0.01 K) to that of the meter plate so as to promote one-dimensional heat flow through the test specimen(s). If the apparatus is located in an environmental chamber, that chamber can be controlled at approximately the mean temperature of the test specimens so that heat gains or losses at the edges of the specimen and the outer edge of the guard plate can be kept acceptably small, affecting the measured properties by less than 0.2 percent. However, for high-temperature apparatus, environmental chambers are normally not used and some form of edge guarding is used with the intention of controlling excessive extraneous heat flows. Most commonly, for a high-temperature circular GHP apparatus, the edge guard is a heated cylinder located coaxially with the hot and cold plates, with edge insulation filling the annulus between the outer edges of the plates and the inner diameter of the edge guard. The major objective of this paper is to examine the effectiveness of this type of edge guarding. First, an analytical solution based on an effective heat transfer coefficient at the edge of the specimen(s) is summarized. Second, analysis is made and computations are carried out to illustrate that, for the type of high-temperature edge guarding that is most commonly used, there can be very significant heat flows in the edge insulation that are not predicted by previous analytical models but that can lead to serious errors in the measured thermal transmission properties. Third, computations based on finite element analyses are presented to show the effectiveness of edge guarding for geometries that are more complex than can readily be handled with analytical solutions. For existing apparatus, the presence of significant shunting heat flows can be confirmed by running tests on specimens of the largest thickness of interest at the same mean temperature, but with very different temperature drops across the specimens.

Daniel R. Flynn, *MetSys Corporation*, P.O. Box 317, Millwood VA 22646, U.S.A.
William M. Healy and Robert R. Zarr, National Institute of Standards and Technology,
Gaithersburg MD 20899-0863, U.S.A.

INTRODUCTION

The guarded hot plate apparatus is generally recognized as the primary absolute method for measurement of the thermal transmission properties of homogeneous insulation materials in the form of flat slabs. This steady-state test method has been standardized by ASTM International as ASTM Standard Test Method C 177 [1] and by the International Organization for Standardization (ISO) as ISO 8302 [2], with the two test methods being similar, but not identical. The first guarded hot plate built in America (*circa* 1912-1914) was designed by Hobart C. Dickinson and Milton S. van Dusen of the National Bureau of Standards (NBS), the former name of the National Institute for Standards and Technology (NIST). A somewhat different guarded hot plate apparatus was independently designed in Germany at about the same time by Robert Poensgen of the Technical University of Munich. Several different guarded hot plate apparatus were built at NBS between 1912 and about 1928. In 1945, the first version of ASTM Test Method C 177, based primarily upon the NBS designs, was approved. Zarr has documented the history of the development of guarded hot plate apparatus at NBS and NIST over the course of the twentieth century [3-4]. The designs and properties of other guarded hot plate apparatus around the world have been described by Pratt [5] and by Klarsfeld [6]. A “reference guarded hot plate apparatus,” based on ISO 8302, has been described by de Ponte *et al.* [7].

A typical guarded hot plate apparatus consists of a square or circular meter plate, surrounded by a coplanar guard plate with a narrow gap between the two plates. A thermopile, with junctions on both sides of the guard gap, is used to control the temperature of the guard plate to be very nearly the same as the temperature of the meter plate. Typically, a pair of similar specimens is tested, one on each side of the guarded hot plate. Heat flows from the hot plate through both specimens to the two cold plates, which, for use over a temperature range from, say, 200 K to 400 K, are usually kept at the same temperature by means of a circulated liquid. Ideally, all of the heat from the meter plate heater flows only through the meter area (i.e., an area equal to the area of the meter plate plus half of the area of the guard gap between the meter plate and the guard plate) of the specimens. In many guarded hot plate apparatus used at moderate temperatures, the equipment is inside an environmental chamber, whose temperature can be adjusted to be nearly equal to the average temperature of the test specimens. By this means, with or without the use of edge insulation, measurement errors due to heat gains to or losses from the edge of the guard plate and the specimens can be kept acceptably small. In some apparatus, a secondary guard plate, outside of the primary guard plate, is used.

Figure 1 shows the overall layout of a typical high-temperature guarded hot plate apparatus. The (usually cylindrical but sometimes square) “stack” is symmetrical about the mid-plane of the apparatus. Each “cold plate,” which in fact may be quite hot but is cold as far as the specimen is concerned, is provided with an electrical heater and is controlled to the desired cold-side temperature. The auxiliary insulation between each cold plate and the corresponding coolant plate keeps the heat load to the cold plate heater to a reasonable value. Each coolant plate is cooled by a circulating liquid.

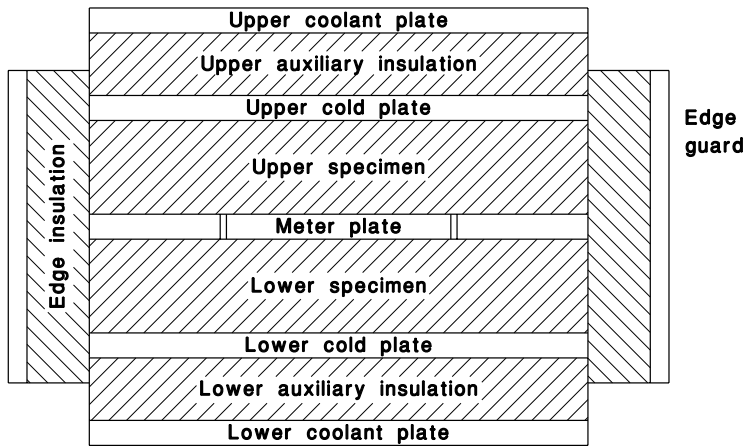


Figure 1 A typical high-temperature guarded hot plate apparatus (cross-section view).

The edge guard, which is significantly larger in diameter than the outer diameter of the stack, is usually controlled at a uniform temperature close to the mean temperature of the specimens. The space between the stack and the edge guard (or guards, if there are separate guards for the two specimens) is filled with insulation.

The edge guard design shown in Figure 1 can lead to very serious errors, e.g., greater than 10 percent in extreme cases. For tests at a high mean temperature, the edges of the guard plate, the two specimens, and the two cold plates will be much hotter than the coolant plates, with the resultant effect that there can be very large longitudinal heat flows in the edge insulation between the stack and the edge guard. The longitudinal heat flow near the stack in this annulus must be provided by radial heat losses from the edges of the cold plates, the edges of the specimens, and even, for thin specimens, from the edge of the guard plate. Thus there can be large net heat losses from the edges of the specimen(s), even when the edge guard is at the mean temperature of the specimen. The problem arises when these edge heat losses become large enough to affect heat flow from the meter plate into the specimens.

PRIOR ANALYSES OF EDGE HEAT LOSS

Several investigators have carried out analyses to compute the estimated error in the measured thermal conductivity or thermal resistance due to the effects of edge heat losses or gains in a guarded hot plate apparatus (GHP). The first such analysis appears to have been that by Van Dusen of NBS [8] for a square apparatus. He assumed the hot plate and the cold plates to be isothermal and the temperature of the outside surfaces of the edge insulation to be the same as the cold plate temperature. The latest version of ASTM C 177 [1] lists references to other analyses of errors due to edge heat loss in guarded hot plate apparatus. In the following section, one particular analysis is summarized and approximate universal curves are generated that permit easy computation of the estimated errors, due to edge heat loss or gain, in measurements made using a GHP, under testing conditions wherein that analysis is appropriate, which certainly may not be the case for high-temperature GHPs similar to the one depicted in Figure 1.

Analysis Based upon Neumann (Convective) Boundary Condition

In 1979, Bode published solutions for the error due to edge heat losses for both square and circular guarded hot plates, with an effective heat transfer coefficient governing the edge heat loss to an arbitrary ambient temperature [9-10]. Peavy and Rennex of NBS had independently developed solutions that were almost identical to those of Bode, but generalized to the case of anisotropic specimens – their work was not published until 1986 [11]. In their paper, they give extensive figures showing the fractional errors due to edge-heat-loss to be expected under various circumstances. Following Peavy and Rennex, the error due to edge heat loss or gain in a guarded hot plate apparatus, of either circular or square geometry, is given by

$$\varepsilon = A + BX, \quad \text{where} \quad X = \frac{2(T_m - T_a)}{T_h - T_c}, \quad (1)$$

in which T_h is the hot plate temperature, T_c is the cold plate temperature, the mean temperature is $T_m = (T_h + T_c)/2$, and T_a is the ambient temperature with which heat is exchanged at the edge of the specimen. For circular geometry, the only case considered in this paper, the coefficients A and B are given by

$$A = \sum_{n=2,4,6,\dots}^{\infty} W_n \quad \text{and} \quad B = \sum_{n=1,3,5,\dots}^{\infty} W_n, \quad (2)$$

where for A the summation is only over even values of n and for B it is only over odd values of n . The terms in the summations are given by

$$W_n = \frac{4}{\pi^2} \left(\frac{h\ell}{\lambda} \right) \left(\frac{\gamma\ell}{b} \right) \frac{I_1(n\pi b/\gamma\ell)}{n^2 [I_1(n\pi d/\gamma\ell) + I_0(n\pi d/\gamma\ell)], \quad (3)$$

where I_0 and I_1 are modified Bessel functions of the first kind of order 0 and 1, respectively; b is the radius of the meter plate to the center of the guard gap; d is the outer radius of the guard ring; ℓ is the thickness of the specimen under consideration; h is the heat transfer coefficient controlling the heat loss or gain at the outer circumference of the specimen; the anisotropy ratio, γ , for the test specimen is defined by $\gamma^2 = \lambda_r/\lambda_z$, the ratio of the thermal conductivity of the specimen in the radial direction to the thermal conductivity in the longitudinal direction; and $\lambda = (\lambda_z\lambda_r)^{1/2}$ is the geometrical mean of the thermal conductivities in the two directions. For the range of parameters that provide good guarding, Eqs. (2) are quite convergent and only a few terms are required to obtain accurate results. Peavy and Rennex [11] provide numerous plots of A and B as functions of geometry and of the ratio of heat transfer coefficient, h , to specimen thermal conductivity.

Returning to Eq. (1), it is important to note that the error due to edge heat loss depends strongly on the ratio of (1) the difference between the effective ambient temperature (or edge guard temperature) and the mean specimen temperature to (2) the temperature difference across the specimen. A consequence of this dependence is that it is more difficult to control edge heat loss effects at high specimen temperatures than it is near room temperature since it is harder to control and measure the effective ambient or edge-guard temperature at high temperatures. Accordingly, it is good practice to use larger temperature differences across the

specimen at high temperatures than would be used near room temperature. Also, a good way to determine experimentally the effects of edge heat loss is to run tests at the same mean specimen temperature but with different temperature differences across the specimen.

As previously developed by the first author of this paper, and documented in ASTM C 1043 [12], for relatively small values of A and B , approximate, but good, universal curves can be obtained by writing

$$A = \frac{h\ell/\lambda}{1 + (1 + \gamma\ell/4\pi d)(h\ell/2\pi\lambda)} \bullet A' \text{ and } B = \frac{h\ell/\lambda}{1 + (1 + \gamma\ell/2\pi d)(h\ell/\pi\lambda)} \bullet B', \quad (4)$$

where A and B are computed from Eqs. (2) and A' and B' are then computed using Eqs. (4). ASTM C 1043 presents curves of A' and B' as functions of $\gamma\ell/d$, with d/b as a parameter. A' and B' are, aside from a very small dependence on $h\ell/\lambda$, functions of $\gamma\ell/d$ and d/b . For a given guarded hot plate, with fixed b and d , the values of A' and B' are, again neglecting the weak dependence on $h\ell/\lambda$, functions only of $\gamma\ell$. The quantities multiplying A' and B' in Eqs. (4) are, aside from a small dependence on $\gamma\ell/d$, functions only of $h\ell/\lambda$ and thus do not depend on the guard radius and meter section radius of the guarded hot plate. For fixed hot- and cold-side temperatures, the quantity X , in Eqs. (1) is a function of T_a , the ambient temperature with which the specimen edges exchange heat. Thus, for a given guarded hot plate, with fixed b and d , the error due to edge heat losses or gains is dependent upon $\gamma\ell$, $h\ell/\lambda$, and T_a , and the dependencies upon these three quantities are easily separable. If one is designing a new guarded hot plate, the values of b and d can also be varied in order to obtain acceptably small edge-effect errors for the specimen thermal conductivities and thicknesses of interest. For example, for the new GHP apparatus being fabricated at NIST, the radius of the meter plate is 100 mm, the radius of the guard plate is 250 mm, and there is 10 mm of insulation between the outer radius of the specimen and the inner radius of the edge guard. Assuming that the edge insulation is isotropic and has the same thermal conductivity as the specimen, the dimensions just given result in $A = 0.000050$ and $B = 0.0122$ for a specimen that is 100 mm thick, the largest thickness that the apparatus can accommodate. In order for the error predicted by Eq. (1) to be less than 0.2 percent, it is necessary for X to be less than 0.16. Thus if the temperature difference would be 20 K, it would be necessary for the edge guard temperature to be within 1.6 K of the mean temperature of the specimen. In designing the apparatus, assumptions were made as to how well the edge guard temperature could be measured and controlled and then the meter plate radius and the thickness of the edge insulation were computed.

ANALYSIS OF “THERMAL SHUNTING” IN EDGE INSULATION

In the present section, examination is made of heat flows in the annular space, which is filled with insulation, between the “stack” (hot plate, specimens, cold plates, auxiliary insulation, and coolant plates) and the coaxial edge guard. For purposes of analysis, it is assumed that the edge guard extends to the outer surfaces of the coolant plates. The edge-insulation region in which heat flow is to be analyzed is $0 \leq z \leq w$ and $a \leq r \leq b$, as shown in Figure 2. It is assumed that the

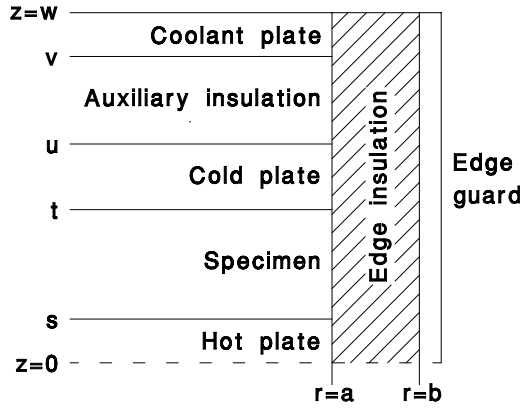


Figure 2. Geometry for shunting analysis.

temperature distribution in the lower half of the edge insulation is the same as that in the upper half so that $z = 0$ is a plane of symmetry. Because of the large range of temperatures from that of the coolant plates to that of the hot plate, the analysis allows the thermal conductivity, $\lambda_e = \lambda_e(\theta)$, of the edge insulation to be a function of temperature so that the temperature distribution in the edge insulation must satisfy the partial differential equation,

$$\nabla \cdot (\lambda_e \nabla \theta) = 0. \quad (5)$$

In order to linearize this equation, a Kirchhoff transformation [13-15] is used. A new potential, or pseudo-temperature, ϕ , is defined as

$$\phi(\theta) = \frac{1}{\lambda_{e0}} \int_0^\theta \lambda_e(\theta') d\theta', \quad (6)$$

where $\lambda_{e0} = \lambda_e(0)$. Applying the Laplacian operator to Eq. (6), comparing the results to Eq. (5), and assuming angular symmetry, it is seen that $\nabla^2 \phi = 0$, so that the partial differential equation has been made linear.

The boundary conditions for the edge-insulation region are taken as

$$0 \leq z \leq w \quad r = a \quad \phi = g(z) \quad (7a)$$

$$0 \leq z \leq w \quad r = b \quad \phi = h(z) \quad (7b)$$

$$z = 0 \quad a \leq r \leq b \quad \frac{\partial \phi}{\partial z} = 0 \quad (7c)$$

$$z = w \quad a \leq r \leq b \quad \phi = g(w) + [h(w) - g(w)] \frac{\ln(r/a)}{\ln(b/a)} \quad (7d)$$

where $g(z)$ is the longitudinal temperature distribution along the outside of the stack, and $h(z)$ is the longitudinal temperature distribution along the inside of the edge guard. The adiabatic boundary condition, Eq. (7c), at the mid-plane, $z = 0$, follows from symmetry. The boundary condition, Eq. (7d), at the outside edge of the coolant plate corresponds to radial heat flow in a metal enclosure or shell that has a high thermal conductivity. The boundary condition at that axial position, $z = w$, is not very important since the details of heat flow there would have little effect on the heat flow into or out of the edge of the specimen. In many cases, the temperature along the plane $z = w$ will be constant at a value near to room temperature so the assumption of temperature being a logarithmic function of the radius does not matter.

The analytical solution that satisfies the above boundary conditions is

$$\phi = g(w) + [h(w) - g(w)] \frac{\ln(r/a)}{\ln(b/a)} + \sum_{n=1,3,5,\dots}^{\infty} \frac{A_n F_0(n\pi r/2w; n\pi b/2w) - B_n F_0(n\pi r/2w; n\pi a/2w)}{F_0(n\pi a/2w; n\pi b/2w)} \cos \frac{n\pi z}{2w}, \quad (8)$$

$$\text{where} \quad F_0(x; y) \equiv I_0(x) K_0(y) - K_0(x) I_0(y), \quad (9)$$

with K_i being the modified Bessel function of the second kind of order i . In the summation in Eq. (8), A_n and B_n are the coefficients of the cosine series describing the longitudinal temperatures distributions at $r = a$ and $r = b$, respectively, and are given by

$$A_n = \frac{2}{w} \int_0^w [g(z) - g(w)] \cos \frac{n\pi z}{2w} dz \quad \text{and} \quad B_n = \frac{2}{w} \int_0^w [h(z) - h(w)] \cos \frac{n\pi z}{2w} dz. \quad (10)$$

At $r = a$ and $r = b$, the terms in the summation in Eq. (8) reduce to simply $A_n \cos(n\pi z/2w)$ and $B_n \cos(n\pi z/2w)$, respectively.

The heat flux into the edge insulation at $r = a$ is

$$q|_{r=a} = -\lambda_e(\theta) \frac{\partial \theta}{\partial r} \Big|_{r=a} = -\lambda_{e0} \frac{\partial \phi}{\partial r} \Big|_{r=a} = -\lambda_{e0} \left(C_0 + \sum_{n=1,3,5,\dots}^{\infty} C_n \cos \frac{n\pi z}{2w} \right), \quad (11)$$

$$\text{where} \quad C_0 = \frac{h(w) - g(w)}{a \ln(b/a)} \quad (12)$$

$$\text{and} \quad C_n = \frac{(n\pi a/2w) A_n F_1(n\pi a/2w; n\pi b/2w) - B_n}{a F_0(n\pi a/2w; n\pi b/2w)}, \quad (13)$$

$$\text{where} \quad F_1(x; y) \equiv I_1(x) K_0(y) + K_1(x) I_0(y). \quad (14)$$

Two specific cases will be considered for the longitudinal temperature distribution along the edge guard. If (Case 1) the longitudinal temperature distribution matches the one along the stack, then $B_n = A_n$ and $C_0 = 0$. If (Case 2) the edge guard is isothermal so that $h(z) = h(w)$ is a constant, then $B_n = 0$.

The longitudinal temperature distribution along the outside of the stack, $r = a$, is taken to be the same as if there were no heat flow across that boundary. Then the heat flow, under that assumption, between the stack and the edge insulation is used to estimate the heat flows in the specimen and thus the error due to edge heat flows. While this analysis is approximate, it provides reliable estimation as to whether or not significant errors exist. The hot plate, cold plate, and coolant plate are each assumed to have a sufficiently high thermal conductivity that they can be considered to be isothermal at temperatures θ_1 , θ_2 , and θ_3 , respectively. Assuming that the specimen and the auxiliary insulation have thermal conductivities that vary with temperature similarly to that of the edge insulation, it is better to assume that ϕ , rather than θ , varies linearly across the specimen and across the auxiliary insulation, so that the potential, or pseudo-temperature, distribution along the stack is described by

$$g(z) = \begin{cases} 0 \leq z \leq s & \phi = \phi_1 \\ s \leq z \leq t & \phi = \phi_1 + (\phi_2 - \phi_1) \frac{z-s}{t-s} \\ t \leq z \leq u & \phi = \phi_2 \\ u \leq z \leq v & \phi = \phi_2 + (\phi_3 - \phi_2) \frac{z-u}{v-u} \\ v \leq z \leq w & \phi = \phi_3 \end{cases}, \quad (15)$$

where ϕ_1 , ϕ_2 , and ϕ_3 correspond to θ_1 , θ_2 , and θ_3 , respectively, and are obtained from those temperatures via Eq. (6). Substituting Eqs. (15) into the first of Eqs. (10) and integrating,

$$A_n = \frac{2}{w} \left\{ (\phi_1 - \phi_3)G(0, s) + \left[\phi_1 - \frac{s(\phi_2 - \phi_1)}{t-s} - \phi_3 \right] G(s, t) + \frac{\phi_2 - \phi_1}{t-s} H(s, t) \right. \\ \left. + (\phi_2 - \phi_3)G(t, u) + \left[\phi_2 - \frac{u(\phi_3 - \phi_2)}{v-u} - \phi_3 \right] G(u, v) + \frac{\phi_3 - \phi_2}{v-u} H(u, v) \right\}, \quad (16)$$

where

$$G(x, y) = \frac{2w}{n\pi} \left(\sin \frac{n\pi y}{2w} - \sin \frac{n\pi x}{2w} \right), \quad (17)$$

and

$$H(x, y) = \frac{4w^2}{n^2\pi^2} \left(\cos \frac{n\pi y}{2w} - \cos \frac{n\pi x}{2w} \right) + \frac{2w}{n\pi} \left(y \sin \frac{n\pi y}{2w} - x \sin \frac{n\pi x}{2w} \right). \quad (18)$$

The above analysis should provide a reasonably accurate evaluation of the heat flow into the edge insulation provided that such heat flow does not result in a large change in the longitudinal temperature distribution along the stack. As indicated in the text following Eq. (14), two specific cases are considered for the longitudinal temperature along the edge guard.

The following analysis was carried out to provide an estimate of the error in the measured thermal conductivity of the specimen due to the heat flow from the edge of the specimen into the edge insulation. It is assumed that the specimen and the edge insulation have thermal conductivities with the same temperature dependence. Assuming the hot plate to be isothermal at $\phi = \phi_1$ and the cold plate to be isothermal at $\phi = \phi_2$, the potential distribution in the specimen can be described by

$$\phi = \phi_1 + (\phi_2 - \phi_1) \frac{x}{\ell} - \frac{\ell}{\pi} \sum_{k=1}^{\infty} D_k \frac{I_0(k\pi r/\ell)}{k I_1(k\pi a/\ell)} \sin \frac{k\pi x}{\ell}, \quad (19)$$

where $x = z - s$, $\ell = t - s$, and the summation vanishes at $x = 0$ and $x = \ell$. The radial heat flux at $r = a$ is

$$q|_{r=a} = -\lambda_{s0} \sum_{k=1}^{\infty} D_k \sin \frac{k\pi x}{\ell}, \quad (20)$$

where λ_{s0} is the thermal conductivity of the specimen at $\phi = 0$. Equating Eqs. (11) and (20) and invoking orthogonality,

$$D_k = \frac{\lambda_{e0}}{\lambda_{s0}} \left[\frac{4C_0}{k\pi} + \sum_{n=1,2,3\dots}^{\infty} C_n \cdot G_{nk} \right], \quad k \text{ odd, and } D_k = \frac{\lambda_{e0}}{\lambda_{s0}} \sum_{n=1,2,3\dots}^{\infty} B_n \cdot G_{nk}, \quad k \text{ even,} \quad (21)$$

where

$$G_{nk} = -\frac{1}{\pi} \left[\cos \frac{n\pi s}{2w} \left(\frac{\cos(k-n\ell/2w)\pi-1}{k-n\ell/2w} + \frac{\cos(k+n\ell/2w)\pi-1}{k+n\ell/2w} \right) \right. \\ \left. + \sin \frac{n\pi s}{2w} \left(\frac{\sin(k-n\ell/2w)\pi}{k-n\ell/2w} - \frac{\sin(k+n\ell/2w)\pi}{k+n\ell/2w} \right) \right]; \quad (22)$$

the terms where the argument of the trigonometric functions is $k-n\ell/2w$ become indeterminate for very small values of that argument, but this problem is easily handled by expanding the terms in series form, thus removing the indeterminacy. The axial heat flux at the surface of the hot plate is, by differentiation of Eq. (19),

$$-\lambda_{s0} \frac{\partial \phi}{\partial x} = \lambda_{s0} \left(\frac{\phi_1 - \phi_2}{\ell} + \sum_{k=1}^{\infty} D_k \frac{I_0(k\pi r / \ell)}{I_1(k\pi a / \ell)} \right). \quad (23)$$

Taking the radius of the meter plate as c , the power input from the meter plate into the specimen is

$$Q_h = \frac{\pi c^2 \lambda_{s0} (\phi_1 - \phi_2)}{\ell} \left[1 + \frac{2\ell^2}{\pi c (\phi_1 - \phi_2)} \sum_{k=1}^{\infty} D_k \frac{I_1(k\pi c / \ell)}{k I_1(k\pi a / \ell)} \right], \quad (24)$$

where the equation has been written so that the second term within the square brackets represents the fractional error in the measured thermal conductivity due to edge heat loss from the specimen.

Calculations based on the above analysis were carried out for a hypothetical apparatus with the stack being 500 mm in diameter (the size of the new apparatus being built at NIST) and the inside diameter of the edge guard being 600 mm, so that the annulus between the stack and the edge guard was 50 mm wide. Dimensions were purposely chosen so as to demonstrate a large effect due to shunting heat flow in the edge insulation. The thickness of the hot plate was taken as 16 mm, the thickness of the specimen was 100 mm (the largest thickness for which the new NIST GHP was designed) and the thicknesses of the cold plate, the auxiliary insulation, and the coolant plate were each taken as 10 mm. The test specimens, the auxiliary insulation, and the edge insulation filling the annulus were all assumed to have a thermal conductivity that varies linearly with temperature according to the equation $\lambda = 0.030[1 + 0.0035(T - 273.2)]$ W/(m·K), which is fairly typical of a fiberglass board in air. For this computation, the mean temperature of the test specimens, as well as the temperature of the isothermal edge guard, was taken as 900 K, the temperature difference across the test specimens was 10 K, and the coolant plate was at 300 K. The upper left-hand drawing in Figure 3 shows the temperature distribution along the stack (Eq. (15)) while the lower left-hand drawing shows the corresponding heat flux (Eq. (11)) from the stack into the edge insulation for the test conditions described above. The right-hand drawings in Figure 2 are expanded versions of the left-hand drawings, so as better to show the temperature distribution and heat flux for the hot plate and, especially, for the

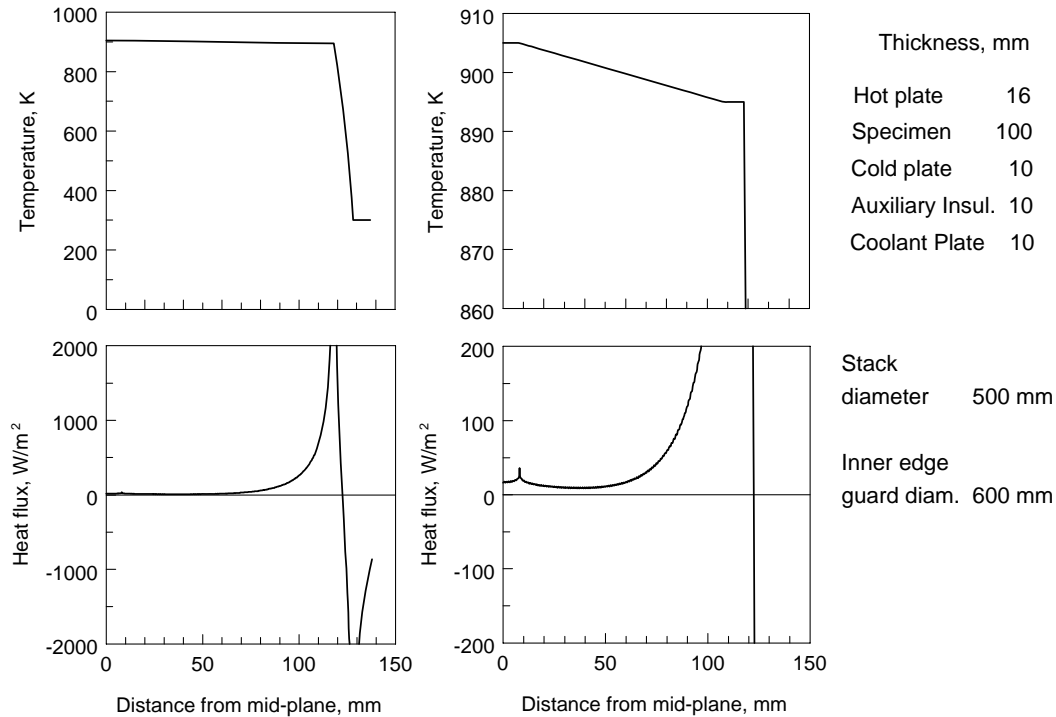


Figure 3. Temperature distribution along the edge of the stack and the heat flux from the stack into the edge insulation for an isothermal edge guard. The left and right drawings show the same curves but with different scales for the vertical axes.

specimen. Looking at the upper drawings of Figure 3, the assumed temperature distribution is seen to be uniform at 905 K through the meter plate, to drop across the specimen, to be uniform at 895 K in the cold plate, to drop very sharply across the auxiliary insulation, and to be uniform at 300 K in the coolant plate. Looking now at the lower drawings of Figure 3, it is seen that from the guard plate and from the hotter half of the test specimen there is heat flow out of the stack into the edge insulation. Some of this heat flow is radial heat loss to the edge guard. However, as z approaches the interface between the hot plate and the specimen, there is an increase in the heat flux because heat must flow into the edge insulation in order to sustain there a longitudinal temperature gradient corresponding to that in the specimen. In effect, there is a shunting heat flow in the edge insulation adjacent to the stack and that heat must be provided by, or given up to, the stack. As z approaches the interface with the auxiliary insulation, there is a very large heat flow into the edge insulation in order to support the steep temperature gradient next to the auxiliary insulation. Heat flows from the edge guard into the stack as z approaches the location of the isothermal coolant plate. In order better to compare the results from the shunting analysis with the results from the more traditional convective heat loss analysis, the computed heat flux distribution, along the thickness of the specimen only, from the shunting analysis is shown in Figure 4 plotted on a logarithmic scale as the solid line labeled “shunting.” The left edge of the graph corresponds to the hot side of the specimen and the right edge to the cold side. The two lower dashed curves were computed using the analysis for convective heat exchange, with radial heat flow from the edge of the specimen to

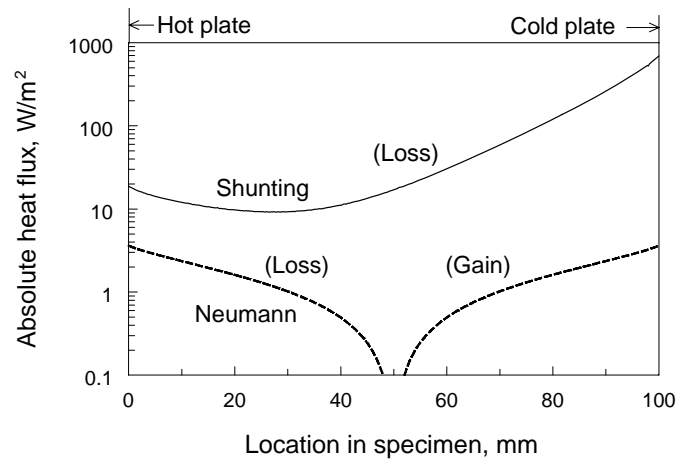


Figure 4. Heat flux from the stack into the edge insulation as predicted by the Neumann (convective) analysis and by the shunting analysis for the same dimensions as shown on Figure 3. The mid-plane of the specimen is at 50 mm.

the isothermal edge guard. The left dashed curve represents a heat loss from the specimen to the edge guard that decreases to zero at a location near the mid-plane of the specimen. The right dashed curve, shown as the absolute value of the heat flux out of the specimen, is actually the predicted heat gain into the specimen from the edge guard. **The contrast between the upper curve and the lower curves is startling, to say the least!** Near the mid-plane of the specimen, the convective analysis indicates essentially no radial heat flow, while at that location, the shunting analysis indicates a heat flux corresponding to a loss of 17 W/m^2 . At the cold side of the specimen, the convective analysis predicts a heat gain of less than 4 W/m^2 while the shunting analysis predicts a heat loss of 700 W/m^2 . The shunting analysis predicts a heat flux that is almost two hundred times larger, and of the opposite sign, than the flux predicted by the convective analysis.

A series of computations was made for the same conditions as those described in the previous two paragraphs, but with the width of the annulus containing the edge insulation being varied from 0.5 mm to 100 mm. The computations were done both for an isothermal edge guard at the mean specimen temperature and for an edge guard with the same longitudinal temperature distribution as that along the stack. The results are shown in Figure 5, where the ordinate corresponds to the predicted error, computed from Eq. (24), in percent, in the measured thermal conductivity of the specimen, and the abscissa to the thickness of the annulus that contains the edge insulation. As shown in the left-hand drawing in Figure 5, which covers edge insulation thicknesses from 5 mm to 100 mm, the errors due to shunting heat flow in the edge insulation become quite significant when the annulus is relatively wide. For the case of a 50 mm annulus, corresponding to the curves shown in figures 3 and 4, the predicted error is 4.3 % for an isothermal edge guard and 8.1 % for matched guarding. The reason that an extended isothermal edge guard works better than a matched edge guard is that the isothermal guard provides more of the heat needed to establish the longitudinal temperature distribution in the edge insulation. The right-hand drawing in Figure 5 shows the edge-heat-loss error for the two types of guarding when the annulus varies from 0.5 mm to 20 mm. For

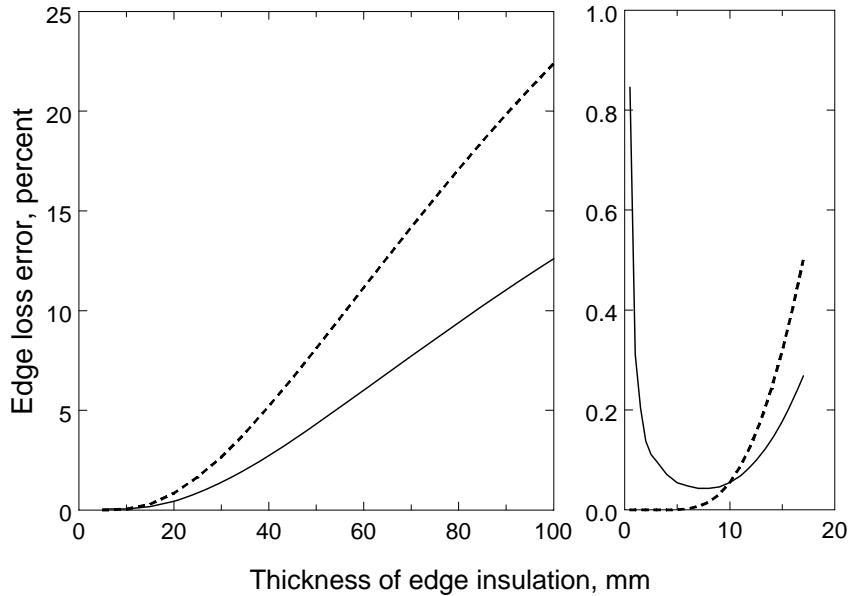


Figure 5. Computed edge-loss error, for both an extended isothermal edge guard and a matching edge guard, as functions of the thickness of the edge insulation. The left-hand drawing corresponds to thicknesses from 5 to 100 mm while the right-hand drawing covers the range from 0.5 to 20 mm.

matched guarding, the error is less than 0.1 % for an annulus thickness of 11 mm or less. For an isothermal edge guard, at the mean specimen temperature, the error decreases with decreasing annulus thickness until the annulus becomes less than 7 mm, and then the error increases with a further decrease in annulus thickness, becoming nearly 1 % for a thickness of 0.5 mm. The error for small annulus thicknesses can be reduced by making the isothermal edge guard temperature slightly higher than the mean temperature of the specimen. If the edge guard temperature is set at 900.03 K, rather than 900.00 K, the computed edge loss error is less than 0.1 % for annulus thicknesses from 13 mm down to 1 mm. However, it would be exceedingly difficult to make the edge guard isothermal to within hundredths of a kelvin and to match the mean edge guard temperature to the mean specimen temperature to within such tight tolerances. Therefore, it would be prudent, for the values of the parameters for these computations, to select an annulus thickness somewhere near 10 mm so that the edge loss error will not be so sensitive to the edge guard mean temperature.

The conditions selected for the computations shown in Figures 4 and 5 were intentionally quite extreme, with very thick specimens and rather thin cold plates and auxiliary insulation, a high mean temperature, and a rather small temperature drop across the specimens. In order to obtain more realistic estimates of the errors that might be encountered due to edge heat loss, computations were made for the same stack diameter, hot plate thickness, meter plate diameter, and insulation thermal conductivity as described above, but increasing the thickness of the cold plates and the auxiliary insulation to 25 mm. The inner diameter of the edge guard was 600 mm, corresponding to an edge-insulation thickness of 50 mm, as was the case for the computed values plotted in Figures 4 and 5. Computation of the edge

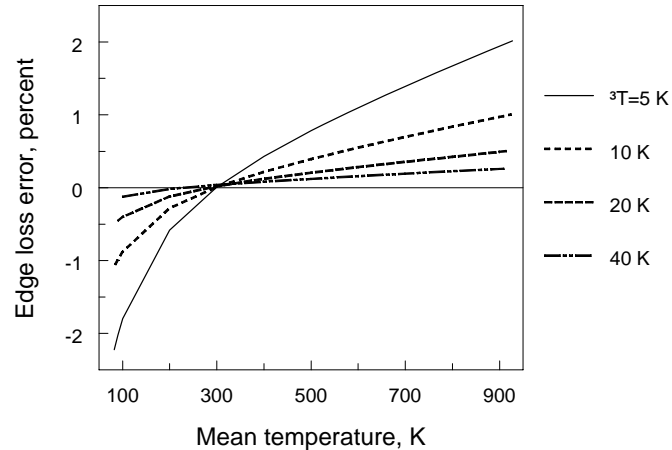


Figure 6. Computed edge-loss error as a function of mean temperature, with differing temperature differences across the specimens, for the conditions described in the text.

loss error (see Eq. (24)) was made for temperature differences across the specimens of 5 K, 10 K, 20 K, and 40 K, at mean temperatures ranging from below 90 K to above 900 K, with the edge guard at that mean specimen temperature, and with the coolant plates held at 300 K. The results, shown in Figure 6, indicate that significant edge loss errors would be expected when the mean temperature of the specimens differs considerably from that of the cooling plate, particularly for smaller temperature differences across the specimens. Additional computational results and a computer program based on the above analysis are available [16-17].

FINITE ELEMENT ANALYSES

As described elsewhere [18-20], the edge-guard configuration for the new NIST GHP is more complex than the simple model assumed for the analysis in the present paper. Finite element analyses were carried out for the geometry and material properties documented in Figure 13 and Table 4 of the paper by Healy and Flynn [19]. These analyses were carried out for two cases having an isothermal edge guard at the mean specimen temperature, one with a 50 mm wide annulus between the stack and the edge guard and one with a 10 mm annulus. Only the case with a 10 mm annulus was discussed in the previous paper [19]. The temperature contours for both cases are shown here in Figure 7. With 50 mm of edge insulation there is significant shunting heat flow from the specimen into the edge insulation, resulting in a serious edge-loss error. By reducing the inside diameter of the edge guard from 600 mm to 520 mm, it is seen that there is little shunting heat flow in the edge insulation. Although it is not evident in the figure, when the annulus is reduced to 10 mm, the computed shunting error is reduced to less than 0.2 % for the case with a 40 K temperature difference across the specimen.

CONCLUSIONS

Traditional analyses based upon a Neumann (convective) boundary condition are suitable for estimating the effects of edge heat flow for guarded hot plates at

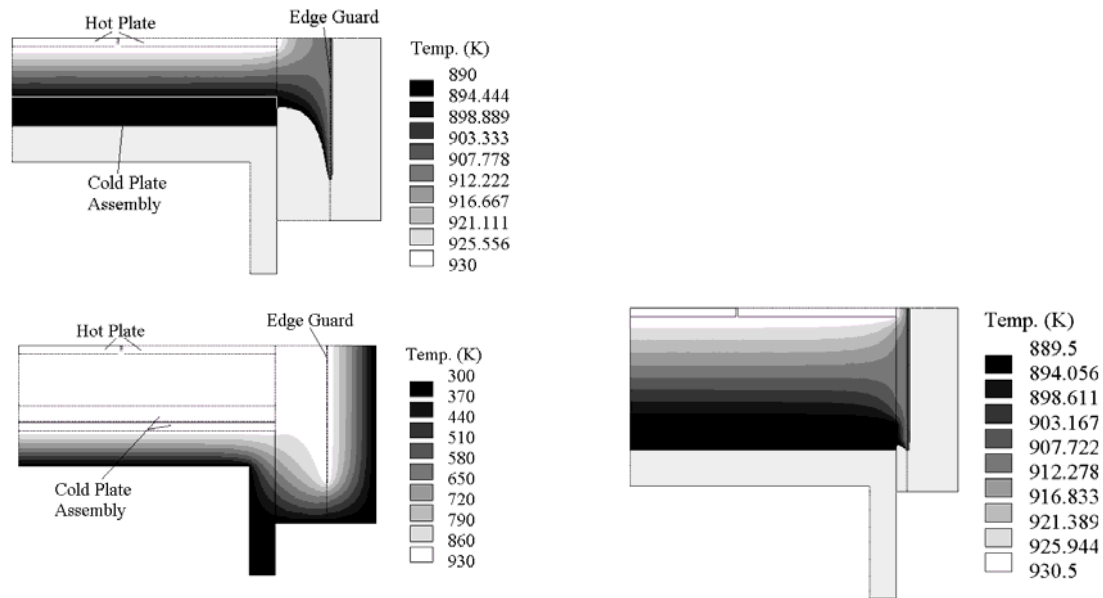


Figure 7. Temperature contours within the specimen and edge insulation for an isothermal edge guard with, on the left, a 50 mm wide annulus and, on the right, a 10 mm annulus.

moderate temperatures if there are no nearby heat sinks or sources at a temperature quite different from that of the test specimens. However, such analyses may drastically underestimate measurement errors due to edge heat flows in high-temperature guarded hot plate apparatus.

Analytical solutions have been presented that provide good estimates of the errors in measured thermal conductivity values due to shunting heat flows in the edge insulation surrounding a high-temperature guarded hot plate apparatus. The results of computations based on these analyses (and confirmed by finite element analysis) have been plotted showing that if the edge insulation is too thick, there may be serious measurement errors due to the effects of shunting heat flow. On the other hand, if the edge insulation is too thin, it may not be practical to match the edge guard temperature closely enough to the desired value to avoid excessive heat exchange between the perimeter of the specimens and the edge guard.

In the design of new guarded hot plate apparatus, it is important to analyze the potential effects of extraneous heat flows in the edge insulation and then to design the apparatus so as to minimize measurement errors due to such heat flows. For existing apparatus, the presence of significant shunting heat flows can be confirmed by running tests on specimens of the largest thickness of interest at the same mean temperature, but with very different temperature drops across the specimens.

REFERENCES

1. ASTM C 177-04, "Standard Test Method for Steady-State Heat Flux Measurements and Thermal Transmission Properties by Means of the Guarded-Hot-Plate Apparatus," *Annual Book of ASTM Standards Vol. 04.06*. West Conshohocken, PA: ASTM Intl.
2. ISO 8302. 1991. "Thermal Insulation – Determination of Steady-State Areal Thermal Resistance and Related Properties B Guarded-Hot-Plate Apparatus", Geneva, Switzerland: Intl. Organization for Standardization.

3. Zarr, R. R. 1997. "History of the Guarded-Hot-Plate Apparatus at NIST," available on the Internet at <<http://www.bfrl.nist.gov/863/hotplate>>, Gaithersburg MD: National Institute of Standards and Technology.
4. Zarr, R. R. June 2001 "A History of Testing Heat Insulators at the National Institute of Standards and Technology," *ASHRAE Trans.* 107, Part 2: 661-671.
5. Pratt, A. W. 1969. "Heat Transmission in Low Conductivity Materials, in *Thermal Conductivity, Vol. 1*, R. P. Tye, ed. London: Academic Press, pp. 301-405.
6. Klarsfeld, S. 1984. "Guarded Hot Plate Method for Thermal Conductivity Measurements," in *Compendium of Thermophysical Property Measurement Methods, Vol. 1, Survey of Measurement Techniques*, K. D. Maglic, A. Cezairliyan, and V. E. Peletsky, eds. New York: Plenum Press, pp. 169-230.
7. de Ponte, F., C. Langlais, and S. Klarsfeld. 1992. "Reference Guarded Hot Plate Apparatus For The Determination Of Steady-State Thermal Transmission Properties," in *Compendium of Thermophysical Property Measurement Methods, Vol. 2, Recommended Measurement Techniques and Practices*, K. D. Maglic, A. Cezairliyan, and V. E. Peletsky, eds. New York: Plenum Press, pp. 99-131.
8. van Dusen, M. S. 1920-21. "The Thermal Conductivity of Heat Insulators," *A. S. R. E. Journal* 7: 202-231.
9. Bode, K.-H.. 1980. "Wärmeleitfähigkeitsmessungen mit dem Plattengerät: Einfluß der Schutzringbreite auf die Meßunsicherheit," *Intl. J. Heat Mass Transfer* 23: 961-970.
10. Bode, K.-H. 1985. "Thermal Conductivity Measurements With The Plate Apparatus: Influence Of The Guard Ring Width On The Accuracy Of Measurements," in *Guarded Hot Plate and Heat Flow Meter Methodology*, C. J. Shirliffle and R. P. Tye, eds., ASTM STP 879, Philadelphia: American Society for Testing and Materials, pp. 29-48. (This paper is an English translation of Ref. 8.)
11. Peavy, B. A., and B. G. Rennex, B.G. 1986 "Circular and Square Edge Effect Study for Guarded-Hot-Plate and Heat-Flow-Meter Apparatuses," *J. Thermal Insulation* 9: 254-300.
12. ASTM C 1043-97, "Standard Practice for Guarded-Hot-Plate Design Using Circular Line-Heat Sources," *Annual Book of ASTM Standards Vol. 04.06*. West Conshohocken PA: ASTM Intl..
13. Van Dusen, M. S. 1930. "Note on the Theory of Heat Conduction," *Bur. Standards J. Research*, 4: 753-756.
14. Carslaw, H. S., and J. C. Jaeger. 1959. *Conduction of Heat in Solids, 2nd Ed.* Oxford: Clarendon Press, pp. 10-11.
15. Özişik, M. N. 1968. *Boundary Value Problems of Heat Conduction*. Scranton, Pa.: Intl. Test Book Co., pp. 353-356.
16. Flynn, D. R. February 2000. "Design of a 500 mm Guarded Hot Plate Apparatus for Measuring Thermal Transmission Properties of Insulations from 90 to 900 K. Phase I – Final Rept," *MetSys Rept. No. 00-02-101*. Reprinted as NIST Grant/Contract Report GCR 05-880, September 2005.
17. Flynn, D. R. December 2003. "Design of a 500 mm Guarded Hot Plate Apparatus for Measuring Thermal Transmission Properties of Insulations from 90 to 900 K. Phase II – Final Rept," *MetSys Rept. No. 03-02-101*. Reprinted as NIST Grant/Contract Report GCR 05-881, September 2005.
18. Flynn, D. R., R. R. Zarr, M. H. Hahn, and W. M. Healy. 2002. "Design Concepts for a New Guarded Hot Plate Apparatus for Use over an Extended Temperature Range," in *Insulation Materials: Testing and Applications: 4th Volume, ASTM STP 1426*, A. O. Desjarlais and R. R. Zarr, eds. West Conshohocken PA: ASTM Intl., pp. 98-115.
19. Healy, W. M. and D. R. Flynn. 2002. "Thermal Modeling of Multiple-Line-Heat-Source Guarded Hot Plate Apparatus," in *Insulation Materials: Testing and Applications: 4th Volume, ASTM STP 1426*, A. O. Desjarlais and R. R. Zarr, eds. West Conshohocken PA: ASTM Intl., pp. 79-97.
20. Zarr, R. R., D. R. Flynn, J. W. Hettenhouser, N. J. Brandenburg, and W. M. Healy. 2005 "Fabrication of a Guarded-Hot-Plate Apparatus for Use over an Extended Temperature Range and in a Controlled Gas Atmosphere," in the proceedings of this conference.